EFFECT OF NEIGHBORING FIBERS ON ENERGY RELEASE RATE DURING FIBER/MATRIX DEBOND GROWTH

L. Zhuang[a,b], A. Pupurs[b,c*]

[a]*Department of Aerospace Engineering, Texas A&M University, College Station, TX-77843, USA*
[b]*Luleå University of Technology, SE 97187 Luleå, Sweden*
[c]*Swerea SICOMP, SE-94129, Piteå, Sweden*

**andrejs.pupurs@ltu.se*

Keywords: fiber breaks, debonding, energy release rate, FEM modeling

Abstract

In this paper fiber/matrix interface debond growth in unidirectional composites subjected to mechanical tensile loading is analyzed using fracture mechanics principles of energy release rate (ERR). The objective of the present study is to analyze the effect of neighboring fibers on the ERR. 5-cylinder axisymmetric FEM models with adjustable inter-fiber distance were used for ERR calculations. The results show that the ERR slightly increases with the inter-fiber distance in the case of long debonds. For short debonds, however, because the stress-state is more complex, it was found that the debond propagates in a mixed Mode I and Mode II and contribution of each mode to the ERR depends on the actual debond length. It was found that for very small debond lengths ERR significantly increases with the inter-fiber distance.

1. Introduction

When unidirectional (UD) composites are loaded in fiber direction in cyclic tension-tension and the tensile load is sufficiently high, multiple fiber breaks occur during the first cycle due to statistical distribution of fiber strength. Once the fiber breaks form, yielding of matrix or fiber/matrix debonding can be expected near the fiber breaks as a result of large shear stresses in the interface region. In the present paper we are focusing on fiber/matrix debonding (interface cracks) initiated at the fiber break and growing along the fiber, which may be the case for relatively weak fiber/matrix interfaces. Interface debond growth leads to progressive degradation of composite properties before the final catastrophic failure of the composite. Hence, quantification of debond crack growth rate in cyclic loading is important. The debond growth in UD polymer composites has been previously analyzed in [1-3] using fracture mechanics principles of energy release rate (ERR). In polymeric composites, due to larger Poisson's ratio and larger coefficient of thermal expansion of the matrix the debond growth was shown to propagate purely in Mode II [1-4] when subjected to tensile loading and negative temperature changes. It was shown in [1-4] with analytical and numerical models that debond growth rate is higher for short debonds due to interaction with fiber break which results in magnification of the ERR. As the debond crack propagates and the debond crack tip advances far away from the fiber break the debond growth becomes self-similar [2,4]. For such case (long debonds) exact analytical models for ERR calculation were developed in [1,3]. In [1-3] a cylindrical unit cell was used consisting of a broken and partially debonded fiber which is surrounded by a matrix cylinder. The effect of the surrounding composite in [1-

3] was represented by an effective composite cylinder surrounding the fiber/matrix concentric cylinder unit cell, see Fig.1.

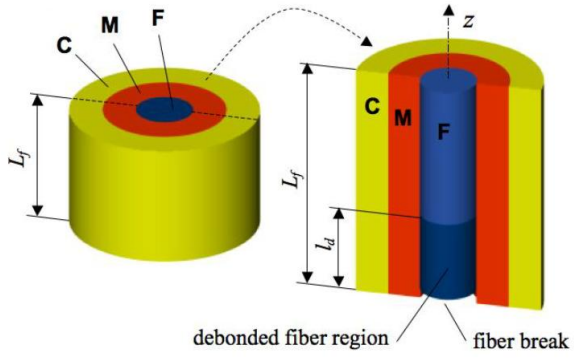

Figure 1. 3-phase concentric cylinder assembly model of a broken and partially debonded fiber in UD composite: F – fiber, M – matrix, C – effective composite.

Calculations in [3] showed that the presence of the effective composite phase in the model is important: ignoring it leads to significantly over-estimated ERR. Despite the accuracy of the analytical models, the previous studies [1-3] have analyzed an idealized geometry without taking into account the possible non-uniformity of the local fiber arrangement which is present in most of the real cases. Certainly, the local microstructure can affect the stress state around the broken fiber and hence it can affect the debond growth rate. The objective of the present paper is to study the effect of the neighboring fibers on debond growth in UD composites. A simple 5-phase concentric cylinder model with variable inter-fiber distance keeping the average volume fraction constant was used to calculate the ERR. FEM software ANSYS [5] was used to perform calculations. Only mechanical tensile loading was studied in the present paper.

2. Self-similar debond growth

2.1. Analytical solution for 3-phase composite

Prior to analyzing the influence of the neighboring fibers on the debond growth, previously obtained results and trends for a 3-phase composite will be briefly reviewed. As it will be shown they provide important information for establishing the geometry for a 5-phase concentric cylinder model used in the present study.

Energy release rate for self-similar debond growth in UD composites with uniform fiber distribution was previously calculated in [1-3] using a 3-phase concentric cylinder model. It was shown in [3] that the ERR for self-similar debond growth can be expressed as a square of a linear combination of applied mechanical strain ε_{mech} and temperature change ΔT as:

$$G_{II} = \frac{E_1^f r_f}{4}\left[k_m^{\infty}\varepsilon_{mech} + k_{th}^{\infty}\left(\alpha_1^c - \alpha_1^f\right)\Delta T\right]^2 \qquad (1)$$

In (1) r_f is the fiber radius, E_1^f is the fiber longitudinal modulus, α_1^c and α_1^f are thermal expansion coefficients of composite and fiber respectively, k_m^{∞} and k_{th}^{∞} are parameters related to mechanical and thermal response respectively. In [3] it was found that their dependence on elastic properties of constituents and volume fraction V_f is weak and the values are very close

to 1. On the other hand, parametric analysis performed in [3] showed significant dependency of the ERR on the size of the effective composite cylinder revealing that a smaller radius of the composite overestimates the ERR. It was found in [3] that the outer radius equal to 10 times the fiber/matrix cylinder assembly radius is sufficient to represent an infinite composite for ERR calculations with FEM. Based on this result the same proportion between the fiber/matrix assembly and the effective composite phase was used in 5 cylinder FEM model in the present study.

2.2. 5-phase composite FEM model for self-similar debonds

To study the effect of the neighboring fibers on the ERR related to debond growth a 5-phase composite model was used in the present study, see Fig.2. The model is 2-D axisymmetric and it is similar to a 4 phase model used in [6] simplifying a hexagonal fiber alignment by a concentric cylinder assembly. The 5-phase axisymmetric model shown in Fig.2 consists of a fiber as a central phase (denoted as F), surrounded by a matrix phase (M), neighboring fiber phase (F), another matrix phase (M) and effective composite phase (C). For the models shown in Fig.2, z is the symmetry axis showing the axial direction and r is the radial direction. In Fig.2 r_f denotes the radius of the central fiber, ID is the arbitrary inter-fiber distance between the central and neighboring fiber cylinder, R is the radius of fiber/matrix unit, R_E is the external radius of the concentric cylinder model including the effective composite phase, dl_d is the length of the model. In all calculations fiber radius was fixed to r_f =4μm, the model length was dl_d =0.5μm, ID was arbitrarily chosen, the radius of the neighboring fiber phase was determined from the condition that it represents the area of 6 fibers surrounding the central fiber in a hexagonal fiber arrangement, radius R of the fiber/matrix unit was determined from the given volume fraction V_f and the previously defined geometry entities. The outer radius of the concentric cylinder model was $R_E = 10 \cdot R$ based on the analysis performed in [3].

As it was shown in [3], for self-similar debond growth the ERR can be calculated from the condition that at fixed applied load F the bonded region with length dl_d (Fig.2a) becomes a debonded region with the same length dl_d (Fig.2b). Hence, the ERR for self-similar debond growth can be found using the potential energy change ΔU as:

$$G_{II} = \frac{\Delta U}{2\pi r_f dl_d} \tag{2}$$

The potential energy difference ΔU due to debond growth by a unit length dl_d is equal to the difference between the additional work (ΔW) performed due to the crack length increase and the change in the strain energy (ΔU_s), i.e.,:

$$\Delta U = \Delta W - \Delta U_s \tag{3}$$

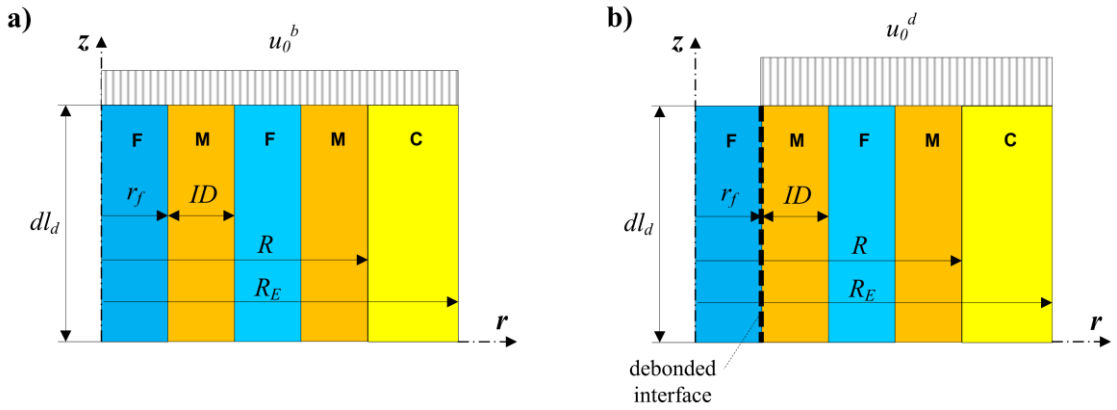

Figure 2. Schematic representation of a 5-phase FEM model: F – fiber, M – matrix, C – effective composite. a) bonded region; b) debonded region.

Additional work due to debond growth by dl_d is equal to:

$$\Delta W = F\Delta u \tag{4}$$

where Δu is the difference between displacements u_0^d and u_0^b in the debonded and bonded regions respectively (see Fig.2a and 2b). To find the displacement difference Δu and the strain energy change ΔU_s necessary for ERR calculation FEM software ANSYS version 13.0 [5] was used. A 2-D model with axisymmetric element behavior was generated. The bonded model (Fig.2a) was generated so that the neighboring areas share the interface line. In the debonded model (Fig.2b) exactly the same geometry as in the bonded model was used, however two coinciding lines were generated on the fiber/matrix interface one belonging to fiber and the other to matrix area. Contact elements were generated on the fiber/matrix interface in the debonded model (Fig.2b). The contact elements were set to comply with pure Lagrange multiplier method which enforces zero penetration when nodes are in contact [5]. Uniform axial displacement was applied on the bonded model as shown in Fig.2a. Reaction force F for the bonded model was calculated and then applied to the 4 phases in the debonded model as shown in Fig.2b. Strain energy for each case was calculated using element table command (ETABLE) in ANSYS [5]. Displacement difference Δu between bonded and debonded models was calculated using simple post-processing. According to the objective of the present study the ERR was calculated for various inter-fiber distances ID.

3. Short debond growth

For short debonds the debond crack tip is close to the fiber break. It was clearly shown in [2] using a 3-phase composite model and in [4] for the single fiber fragmentation test analysis that due to interaction between debond and the fiber break, the ERR for short debond growth is magnified. In the present study the objective is to find the effect of the neighboring fibers on the ERR therefore a 5-phase cylinder assembly model was used. Axisymmetric FEM model schematically shown in Fig.3 was generated in ANSYS [5] to calculate ERR for short debonds. In principle it is very similar to the 5 cylinder model used for self-similar debond ERR calculation (see Fig.2) with the difference that the fiber break is included in the model, the fiber is partly debonded (with debond length denoted as l_d in Fig.3) and the length of the model L_f is significantly larger. A uniform axial displacement u_0 was applied in the FEM model as shown in Fig.3. The ERR was calculated using the virtual crack closure technique (VCCT) routine in ANSYS [5]. VCCT is based on the principle that the energy released due

to crack propagation is equal to the work required to close the same crack surface and that the stress-state near the crack tip is not changing when the increase of the crack length is small. Using VCCT routine in ANSYS allows to obtain the total ERR as well as components of Mode I and Mode II.

The geometrical entities r_f, ID, R and R_E were the same as in the case of self-similar debonds described in Section 2. The length of the FEM model was in all cases $L_f = 200 \cdot r_f$. The ERR was calculated for various debond lengths l_d and inter-fiber distances ID.

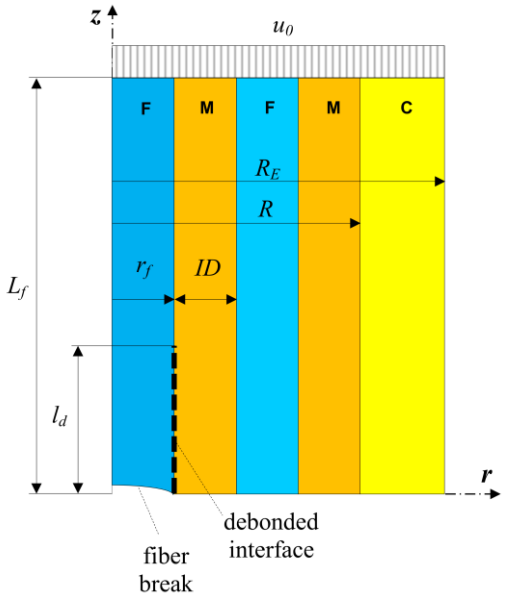

Figure 3. Schematic representation of a 5-phase concentric cylinder assembly FEM model for short debond energy release rate calculations: F –fiber, M – matrix, C – effective composite.

4. Results and discussion

4.1. Material properties

In the present paper a carbon fiber/epoxy composite (denoted as CF/EP) was studied. The elastic properties of the constituents are presented in Table 1. Elastic properties of the effective composite phase were calculated using Hashin's concentric cylinder assembly model [7] and Christensen's self-consistent model [8] for out-of-plane shear modulus. Calculated properties for CF/EP with volume fractions V_f =0.6 and V_f =0.4 are presented in Table 2.

Material	E_1 [GPa]	E_2 [GPa]	ν_{12} [-]	G_{12} [GPa]	ν_{23} [-]	α_1 [1/°C]	α_2 [1/°C]
CF	500	30	0.20	20	0.45	$-1 \cdot 10^{-6}$	$7.8 \cdot 10^{-6}$
EP	3.5	3.5	0.40	1.25	0.40	$60 \cdot 10^{-6}$	$60 \cdot 10^{-6}$

Table 1. Elastic properties of constituents. CF – carbon fiber, EP – epoxy matrix.

V_f [-]	E_1 [GPa]	E_2 [GPa]	ν_{12} [-]	G_{12} [GPa]	ν_{23} [-]	G_{23} [GPa]	α_1 [1/°C]	α_2 [1/°C]
0.6	301.4422	11.0389	0.2734	4.0625	0.5432	3.5767	$-0.6631 \cdot 10^{-6}$	$35.8513 \cdot 10^{-6}$
0.4	202.1433	7.5694	0.3133	2.6136	0.5899	2.3803	$-0.2842 \cdot 10^{-6}$	$50.9694 \cdot 10^{-6}$

Table 2. Elastic properties of carbon fiber/epoxy composite with volume fractions V_f=0.6 and V_f=0.4.

For the elastic properties listed in tables index 1 corresponds to fiber direction, 2 corresponds to transverse to fiber direction and 3 corresponds to out-of-plane direction. The isotropic epoxy matrix (EP) properties are presented in the same coordinate system in Table 1.

4.2. Effect of the inter-fiber distance on self-similar debond growth

Calculation results showing the effect of the inter-fiber distance on self-similar debond growth ERR are shown in Fig.4. The results correspond to mechanical loading with the strain level of $\varepsilon_{mech} = 0.01$. It was found that in mechanical loading the self-similar debonds grow in pure Mode II, hence notation G_{II} in Fig.4. The horizontal axis in Fig.4 shows the inter-fiber distance normalized with respect to the fiber radius, i.e., $IDn = ID/r_f$, see Fig.2. In Fig.4 results for volume fractions V_f =0.6 and V_f =0.4 are shown. The solid vertical line in Fig.4 indicates the inter-fiber distance that corresponds to uniform hexagonal packing for V_f =0.6. The dashed vertical line in Fig.4 indicates the same for V_f =0.4.

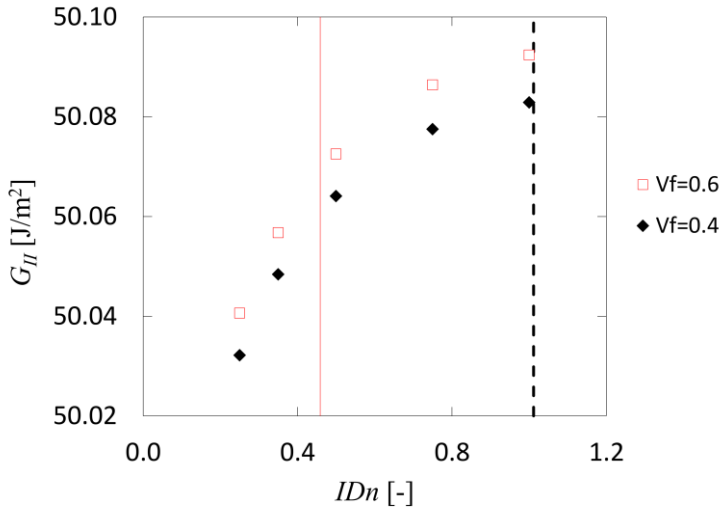

Figure 4. Energy release rate as a function of inter-fiber distance for self-similar debond growth.

In general, results in Fig.4 show that for both studied volume fractions the ERR slightly increases with the inter-fiber distance IDn. The corresponding analytical result for a 3-phase composite obtained using Equation (1) for V_f =0.6 and V_f =0.4 is equal to 50.45 J/m^2 which is higher than the results obtained with a 5-phase composite model in Fig.4.

4.3. Effect of the inter-fiber distance on short debond growth

Calculation results showing the effect of the inter-fiber distance on short debond growth ERR are shown in Fig.5. The results only for volume fraction V_f =0.6 are presented. The results correspond to mechanical loading with the strain level of $\varepsilon_{mech} = 0.01$. The solid vertical line in Fig.5 indicates the inter-fiber distance that corresponds to uniform hexagonal packing for V_f =0.6. Unlike for self-similar debonds which propagate in pure Mode II, for short debonds it was found that in some cases Mode I contribution is significant. The results in Fig.5 show the total ERR, denoted as G, containing both Mode I and Mode II components. ERR is plotted against the normalized inter-fiber distance $IDn = ID/r_f$. Curves corresponding to

different normalized debond lengths $l_{dn} = l_d / r_f$ are presented. The results in Fig.5 show that when the debond length is very small, for example, $l_{dn} = 1$, the ERR significantly increases with the inter-fiber distance IDn. It was also found that for very small debond lengths the contribution of Mode I is larger than for longer debond lengths.

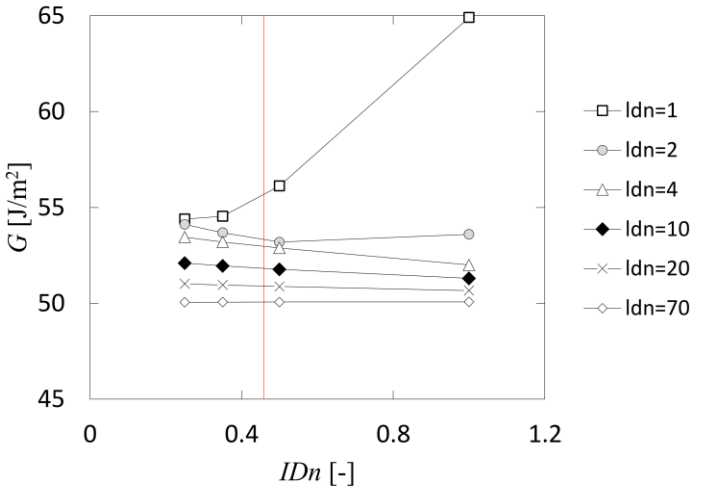

Figure 5. Energy release rate as a function of inter-fiber distance for short debonds.

It was found that for debond lengths $4 \le l_{dn} \le 50$ the ERR decreases slightly with the increase of the inter-fiber distance IDn (see Fig.5). However, when debond length $l_{dn} > 50$, the ERR was found to increase slightly with the inter-fiber distance IDn, which is well consistent with the trends found for self-similar debond growth (see Fig.4)

Another way to analyze results for short debonds is to plot the magnification of ERR as a function of debond length l_{dn} at fixed inter-fiber distance IDn. Such plots are presented in Fig.6. The results plotted in Fig.6 consistently show larger magnification of ERR when the inter-fiber distance IDn is larger.

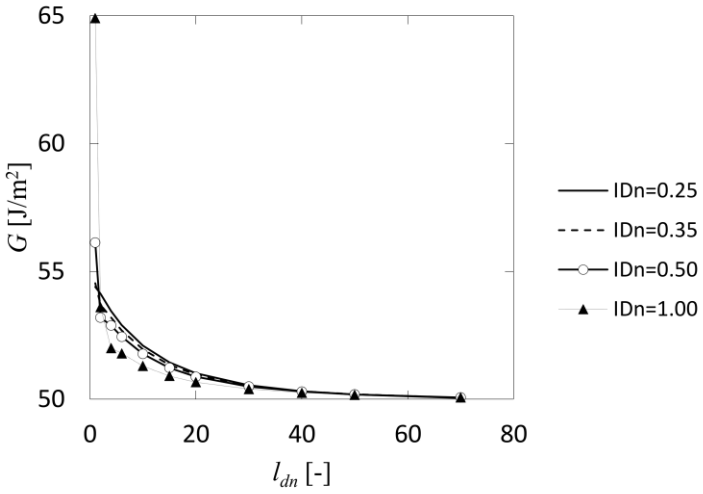

Figure 6. Energy release rate as a function of normalized debond length.

5. Conclusions

The effect of neighboring fibers on the energy release rate (ERR) for debond growth in unidirectional carbon fiber/epoxy composites was analyzed. 5-phase concentric cylinder FEM model was used for calculations. The model consists of a broken fiber embedded in matrix and surrounded by a cylinder of fiber material representing the neighboring fibers with variable distance to the broken fiber. It is followed by a matrix cylinder with outer radius ensuring that the fiber content in the unit is the same as for composite in average. This unit is embedded in the effective composite cylinder. Only mechanical tensile loading was considered. Different FEM models were used for self-similar and for short debond growth analysis. It was found for self-similar debond growth that the ERR slightly increases with the inter-fiber distance and propagation is purely in Mode II. For short debonds, on the other hand, it was found that Mode I contribution to ERR can be significant, especially when debonds are very small. It was found that the ERR can either increase or decrease with the inter-fiber distance depending on the debond length. For shorter debonds it was found that ERR significantly increases with the inter-fiber distance. When the normalized debond length l_{dn} is in the range of $4 \le l_{dn} \le 50$ the ERR slightly decreases with the inter-fiber distance. Finally, it was found that when the debond length $l_{dn} > 50$ the ERR slightly increases with the inter-fiber distance resembling the trend found for self-similar debond growth.

References

[1] A. Pupurs and J. Varna. Energy release rate based fiber/matrix debond growth in fatigue. Part I: Self-similar crack growth. *Mechanics of Advanced Materials and Structures*, 20(4):276-287, 2013.

[2] A. Pupurs, A. Krasnikovs and J. Varna. Energy release rate based fiber/matrix debond growth in fatigue. Part II: Debond growth analysis using Paris law. *Mechanics of Advanced Materials and Structures*, 20(4):288-296, 2013.

[3] J. Varna and A. Pupurs. Analytical solution for energy release rate due to steady-state fiber/matrix debond growth in UD composites. *Composites Science and Technology*, submitted, 2014.

[4] E. Graciani, V. Mantic, F. Paris, J. Varna. Numerical analysis of debond propagation in the single fiber fragmentation test. *Composites Science and Technology*, 69(15-16):2514-2520, 2009.

[5] ANSYS Academic Research, Release 13.0, Canonsburg, Pennsylvania, 2011.

[6] S. W. Case, G. P. Carman, J. J. Lesko. A. B. Fajardo, K. L. Reifsnider. Fiber fracture in unidirectional composites. *Journal of Composite Materials*, 29(2):208-228, 1995.

[7] Z. Hashin. Analysis of composite materials – a survey. *Journal of Applied Mechanics*, 50(3):481-505, 1983.

[8] R. M. Christensen and K. H. Lo. Solutions for effective shear properties in three phase sphere and cylinder models. *Journal of the Mechanics and Physics of Solids*, 27(4):315-330, 1979.